npj | heritage science

Article

https://doi.org/10.1038/s40494-025-01628-8

Degradation condition and microbial analysis of waterlogged archaeological wood from the second shipwreck site on the northwestern continental slope of the South China Sea

Check for updates

Shimin Chu[1,2], Yunqi Li[2], Xueyu Wang[1] ✉, Naisheng Li[1] ✉, Jianzhong Song[3] & Lanying Lin[2]

The No. 2 Shipwreck Site on the northwestern continental slope (1488–1505 AD) is situated on the seabed between Hainan Island and the Xisha Islands in the South China Sea, at a depth of ~1500 m. Numerous wooden logs were discovered inside the shipwreck. This study assessed the degradation status of the waterlogged archaeological wood comprehensively. It also employed modern biotechnological methods to analyze the microbial communities within the wood and its surrounding environment. The results revealed that the waterlogged archaeological wood had experienced varying degrees of degradation. Even seemingly intact wood has undergone significant microstructural and chemical changes. Specifically, the secondary cell walls have been damaged, but the compound middle lamella remains relatively intact. Chemically, the degradation of hemicellulose and cellulose has resulted in a disordered arrangement of cellulose microfibrils, thereby weakening the mechanical properties of the wood cell walls. Additionally, a significant amount of iron salts was detected in some of the waterlogged archaeological wood. The microbial community within the wood was found to be predominantly composed of bacteria, with the Proteobacteria and Bacteroidetes phyla being the dominant groups. It is notable that the microbial community within the waterlogged archaeological wood exhibits a high degree of similarity with the microbial communities present in the surrounding seabed sediments and seawater. In conclusion, while some of the waterlogged archaeological wood has retained a relatively intact macroscopic appearance, its microstructure and chemical composition have undergone significant deterioration. Therefore, future conservation efforts should prioritise reinforcement and de-ironing to preserve the research value of these artifacts.

The archaeological value of waterlogged wood is invaluable, offering insights into ancient materials and manufacturing techniques, crucial for historical understanding[1]. The biodegradation of wood in long-term underwater environments differs significantly from that of wood on land[2]. Significantly, an in-depth study of the deterioration mechanisms of waterlogged archaeological wood and its associated microorganisms is essential, to provide strategies for its preservation and restoration[3].

In recent years, scholars have made significant advances in the assessment of wood deterioration at various scales, from macro to micro[3,4]. Morphological observations facilitate the clarification of wood preservation status and provide direct evidence of microbial degradation of wood[1]. Kim et al.[5] employed confocal laser scanning microscope and transmission electron microscopy (TEM) to explore microbial attacks in waterlogged archaeological rosewood (*Dalbergia* species). By observing the morphological characteristics, it was determined that the primary type of

[1]National Centre for Archaeology, Beijing, China. [2]Research Institute of Wood Industry, Chinese Academy of Forestry, Beijing, China. [3]Hainan Provincial Institute of Cultural Relics and Archaeology, Haikou, China. ✉e-mail: xy.wang@uch-china.com; lineas@126.com

biodegradation observed in waterlogged archaeological wood was soft rot. The relative content of cell wall components is pivotal in determining the physical and mechanical properties of archaeological wood[6]. Wet chemical analysis, a relatively mature technique for chemical composition analysis, has been widely applied in this field. Considering potential intraspecific variations between modern wood specimens and ancient ones, it is recommended that other techniques, such as spectroscopy and thermochemical analysis, be employed in conjunction with the wet chemical analysis to ascertain the extent of degradation[7]. Furthermore, the crystalline structure of cellulose is a crucial indicator in assessing the degree of deterioration of archaeological wood[8]. Guo et al.[9] have demonstrated that the micro-damage observed in archaeological wood was closely related to a fragmentation of both the cellulose crystallite structure and the cellulose microfibrils. Researchers found that slightly degraded wood displayed cellulose crystallites and microfibrils comparable to those in undegraded wood. In contrast, severely degraded wood exhibited the fragmentation of cellulose aggregates and a notable absence of crystallinity. In conclusion, it is essential to undertake a comprehensive assessment of the deterioration of waterlogged archaeological wood from a variety of perspectives in order to gain a full understanding of the issue. Concurrently, the implementation of non-destructive or minimally invasive assessment techniques is of paramount importance in order to minimise the potential damage to cultural relics[10]. Therefore, the integration of these methodologies is crucial for advancing our understanding and preservation of ancient wooden cultural artefacts.

Because of its distinctive chemical composition and structure, wood is particularly vulnerable to microbial invasion from the surrounding environment, leading to degradation[11,12]. In waterlogged archaeological wood, soft rot fungi, which often coexist with erosive bacteria, are a common type of fungus[1]. Soft rot fungi selectively erode the S_2 layer of the cell wall, breaking down the polysaccharide components. This selective erosion results in multiple cavities in the S_2 layer, which appear as circular or nearly circular voids in cross-section[2]. In contrast, the compound middle lamella (CML) is often preserved. Furthermore, waterlogged archaeological wood is frequently susceptible to bacterial degradation, with the primary agents being erosive, tunnelling and cavitation bacteria. Erosive bacteria, showing notable adaptability and tolerance to environmental conditions, erode the wood from the cell cavity to the secondary wall by etching, preferentially decomposing the S_2 and S_3 layers of the cell wall[13]. This process significantly degrades cellulose, while lignin undergoes relatively minor depolymerisation, demethylation and oxidation[14,15]. Following the erosion process, the cross-section of the wood cell wall exhibits a distinctive reticulated pattern, while the lignin-rich middle lamella remains relatively intact[16]. Tunnelling bacteria move within the wood cell wall without being constrained by the direction of the microfibrils[17]. They can move in various directions, primarily degrading the secondary wall, forming tunnels and occasionally penetrating the entire cell wall[18]. Cavitation bacteria have the capacity to degrade polysaccharides, forming rhombic or irregular cavities that are perpendicular to the fibre length direction within the secondary wall. The initial cavities are minute in size, but they subsequently increase in size while retaining their original rhombic configuration. As the wood continues to decompose, neighbouring cavities may coalesce, resulting in the formation of cavities of varying shapes[17]. The microbial communities present in archaeological wood are highly complex, and therefore an in-depth examination of these communities is essential for the understanding of the causes of degradation and the development of effective conservation strategies.

Two shipwrecks from the Hongzhi period of the Ming Dynasty (1488–1505 AD) were discovered on the seabed of the South China Sea, ~150 km southeast of Sanya, near the Xisha Islands (Fig. 1a). Discovered at a depth of ~1500 m with a constant temperature of 3 °C, these shipwrecks represent the first deep-sea discoveries of their kind by Chinese researchers. This breakthrough significantly advances Chinese deep-sea archaeology and contributes to global archaeological knowledge, filling a critical gap in our understanding of ancient maritime routes in the South China Sea and providing new insights into the historical records of the region's Maritime Silk Road. At the No. 2 shipwreck site, estimated to be around 1527 m deep, a large number of wooden logs were found. These uniformly sized and neatly stacked logs were simply processed, cut to a specific length and exhibited a black colour and hard texture (Fig. 1b). The precise location of the hull of the No. 2 shipwreck remains to be determined. An irregularly shaped piece of wood, likely part of the ship's structure, was found among the central log stack.

This study focuses on the logs and an irregular strip of wood found at the No. 2 shipwreck site on the northwestern continental slope of the South China Sea, provides a comprehensive assessment of their basic density (BD), maximum water content (MWC), anatomical structure, chemical composition and mechanical properties of the cell walls through multi-dimensional indicators to deeply analyze the degree of degradation. Further research was conducted on the microbial communities in the wood and its surrounding environment, aiming to elucidate the potential influence of these microorganisms on the wood degradation process. This study provides a scientific basis for assessing the preservation status of submerged wood on the northwestern continental slope of the South China Sea.

Materials and methods

Materials

All the logs within the No. 2 shipwreck site exhibit a visually uniform appearance and maintain structural integrity, with only minor signs of deterioration affecting the outermost layers. In contrast, the smaller, irregular strip of wood, which is suspected to be components of the ship, have experienced more significant decay. To accurately represent the overall condition of the wreck, samples were taken from the well-preserved internal and slightly deteriorated external parts of one of the logs, labelled S1 and S2, respectively (Fig. 1c). Samples from the poorly preserved irregular strip of wood were also taken and labelled S3 (Fig. 1d). The logs and the irregular strip of wood have been identified as *Diospyros ebenum* Koen and *Toona* sp., respectively, with their optical images presented in additional file. The growth rings of *Diospyros ebenum* are indistinct and characterised by a deep black hue. The vessel elements are barely perceptible to the naked eye and are filled with a brownish-black or black gum. The axial parenchyma is notably abundant, predominantly manifesting as a dense apotracheal type. The wood fibres have thick cell walls. The wood rays are primarily heteromorphic and uniseriate. The *Toona* sp. exhibits semi-porous wood characteristics, with vessels in cross sections appearing round or oval. They are mainly observed as single or multiple, with no spiral thickening present. The perforation plates are flat to slightly inclined, and the vessel pitting is characterised by alternate pitting. The axial parenchyma is marked by its paratracheal type, with occasional scattered occurrences. The wood fibres have thin walls, and the wood rays are predominantly composed of multiple rows. The radiological tissues are predominantly of the heteromorphic type I, with a few instances of heteromorphic type II. Modern intact wood samples were obtained as references, labelled R1 for ebony and R2 for *Toona*. Additionally, seabed sediment and bottom seawater were also collected and sampled. These samples were preserved in sterile tubes and transported at low temperatures to the laboratory, where their microorganisms were identified and the samples were labelled S1, S2, S3, E1 and E2, respectively.

Basic physical parameters

At least three wood blocks from each sample were cut to determine the MWC and BD. Before testing, the samples were cleansed with distilled water. The calculation of MWC for each wood block is detailed in Eq. 1.

$$MWC = \frac{m - m_0}{m_0} \times 100\% \quad (1)$$

The BD is calculated using Eq. 2.

$$BD = \frac{m_0}{v_b} \times 100\% \quad (2)$$

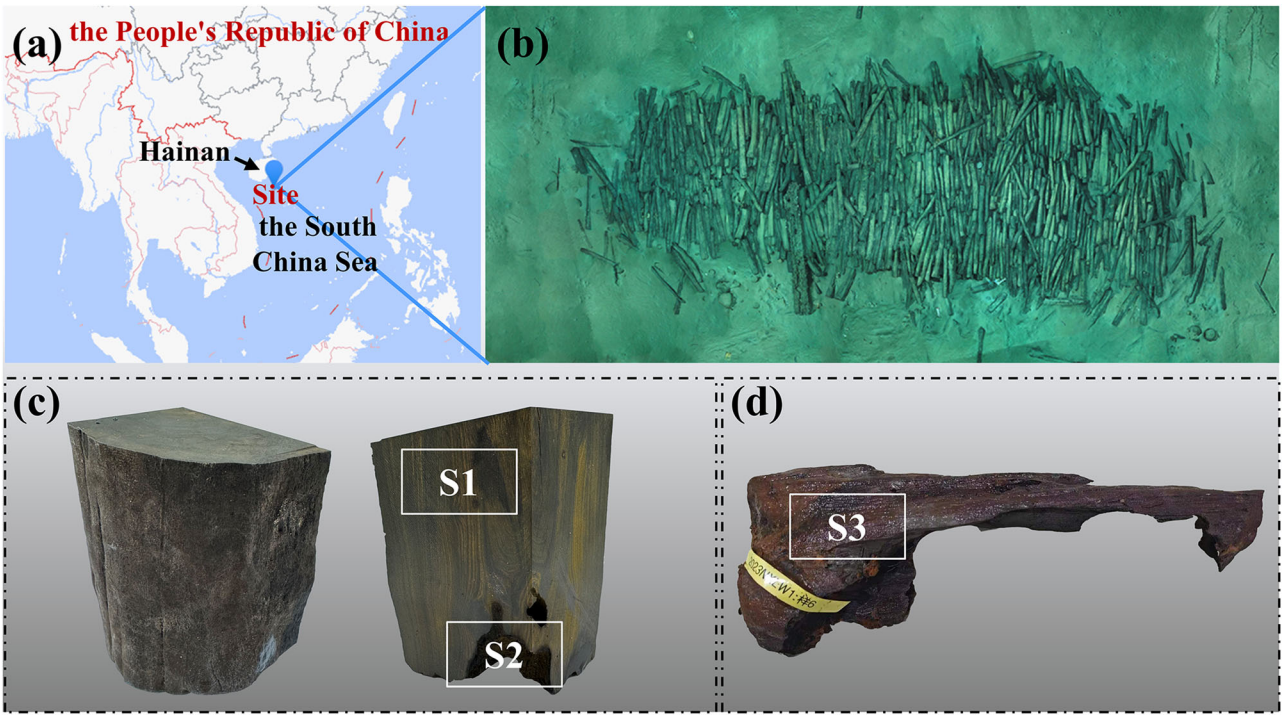

Fig. 1 | The No. 2 shipwreck site on the Northwest Slope of the South China Sea and the collected samples. a Location of the site, **b** Overall view of the site, **c** Waterlogged archaeological ebony, **d** Waterlogged archaeological *Toona* wood.

Where m is the mass of the waterlogged archaeological wood, m_0 is the mass of the oven-dry wood and v_b is the volume of the waterlogged archaeological wood.

Micromorphological structure characteristics

A sliding microtome (SM2010R, Leica, Germany) was employed to flatten the surface of the samples, which were then subjected to freeze-drying. Specimens were mounted on the stage with conductive tape, and a platinum coating was applied to their surface using a sputter coater, enhancing their conductivity. The cross-sectional and longitudinal microstructures of the samples were observed using a field emission scanning electron microscope (SEM) (SU8020, Hitachi, Japan) at an accelerating voltage of 10.0 kV.

To gain further insight into the degradation of waterlogged archaeological wood at the cell wall scale, the freeze-dried archaeological wood was embedded in Spon 812 epoxy resin. Ultra-thin cross-sections, ~60 nm in thickness, were prepared using an ultramicrotome equipped with a diamond knife. Subsequently, the sections were mounted on copper grids, and TEM (HT7800, Hitachi, Japan) was used to observe and capture images at 100 kV.

Chemical characteristics

A Fourier-transform infra-red spectrometer was utilised for the analysis of the chemical composition of waterlogged archaeological wood. Wood samples were ground to a particle size of 120 mesh, dried until a constant weight was achieved at 60 °C, thoroughly mixed with an excess of potassium bromide (KBr) at a mass ratio of 1:100. After mixing, the mixture was then pressed into transparent thin films and subsequently analysed using a Fourier-transform infra-red spectrometer (IS10, Nicolet, America). The spectral analysis covered a range from 4000 cm^{-1} to 400 cm^{-1}, with three replicate measurements per sample group to determine the average spectrum.

The relative content of waterlogged archaeological wood components was determined using the wet chemical method. The wood samples were milled to a particle size of 40-60 mesh. The relative content of extractives, cellulose, hemicellulose and lignin in both archaeological and modern wood was then determined using the extraction, hydrolysis and lignin determination method of Liu et al.[19].

A thermogravimetric (TG) analyser was employed to investigate the correlation between temperature changes and mass changes in waterlogged archaeological wood and reference wood samples. This facilitated a better understanding of the degradation of the chemical components in the waterlogged archaeological wood. The test samples were prepared into a powder with a particle size of 120 mesh, each weighing ~2 mg. The analysis was conducted under a nitrogen atmosphere, with a heating rate of 10 °C/min over a temperature range of 30–800 °C.

An X-ray diffractometer was employed to investigate the cellulose crystalline structure of waterlogged archaeological wood. The wood samples were milled to a particle size of 80 mesh and dried to a constant weight at 60 °C. The crystalline structure of cellulose was then characterised using an X-ray diffractometer (D8 Advance, Bruker, Germany). The instrument was operated with a voltage of 40 kV, current of 40 mA, scanning speed of 1.5°/min, scanning step of 0.05° and scanning range from 5° to 45° for 2θ. Each group of samples was subjected to three trials, and the resulting spectra were averaged to improve the accuracy of the measurements. The crystallinity index of the wood samples was calculated using the empirical method proposed by Segal method (Eq. 3)[20].

$$CrI = \frac{I_{200} - I_{am}}{I_{200}} \times 100\% \quad (3)$$

Where I_{200} represents the maximum diffraction intensity of cellulose at the (200) crystal plane, and I_{am} is the scattering intensity of the background diffraction from the amorphous region of cellulose near 2θ at 18°.

Micromechanical properties

A nanoindentor coupled with a scanning probe microscope was employed to investigate the longitudinal micromechanical properties of the wood fibres within the samples to examine the mechanical properties and loss in archaeological wood at the cellular level. The samples were prepared as small wooden blocks measuring 15 mm by 7 mm by 7 mm and subjected to a freeze-drying treatment. The dried samples' cross-sections were trimmed to squares ~1 mm × 1 mm in size using a single-edged razor blade. The cross-sections were polished using a diamond knife on an

ultramicrotome in order to achieve a smooth surface. A Berkovich diamond indenter with a tip diameter of 100 nm and a pyramidal angle of 142.3° was selected for the investigation. In load control mode, a three-stage loading protocol was applied, consisting of a 5-s loading phase, a 2-s dwell and a 5-s unloading phase, with a maximum load of 120 μN. Each sample group was tested using at least three samples, each with at least 15 test points.

Microbiological testing

The samples, retrieved from sterile tubes, were ground into a fine powder using liquid nitrogen. The Deoxyribonucleic acid (DNA) was extracted from the samples using a soil DNA extraction kit. The genomic DNA was then subjected to 1% agarose gel electrophoresis following the manufacturer's instructions. Polymerase chain reaction was employed to amplify the V3–V4 region of the bacterial 16S rRNA gene (341F: CCTAYGGGRBGCASCAG and 806R: GGACTACNNGGGTATCTAAT) and the internal transcribed spacer region ITS1-ITS2 of fungi (ITS1F: CTTGGTCATTTAGAGGAAGT AA and ITS2R: GCTGCGTTCTTCATCGATGC). High-throughput sequencing was performed on the Illumina MiSeq sequencing platform.

Table 1 | The MWC and BD of waterlogged archaeological wood and reference wood samples

Samples	Maximum moisture content (%)	Basic density (g/cm^3)
S1	22.95 (±1.26)	1.22 (±0.03)
S2	28.69 (±2.39)	1.10 (±0.03)
S3	144.38 (±5.07)	0.43 (±0.02)
R1	19.44 (±1.56)	1.23 (±0.02)
R2	114.19 (±2.77)	0.52 (±0.02)

Results and discussion

Physical properties

Table 1 presents the MWC and BD of waterlogged archaeological wood and reference wood, which are two physical indicators commonly used to assess the degree of degradation of waterlogged archaeological wood[21]. Generally, the MWC for the same tree species tends to increase with increasing degradation of the waterlogged archaeological wood, whereas the BD tends to decrease. The MWC of S1 and S2 were found to be 22.95% and 28.69%, respectively, significantly higher than that of R1 (19.44%), indicating a substantial difference. The MWC of the ebony samples was notably lower compared to values reported for archaeological woods in other studies[12,22,23]. This was mainly due to the large amounts of gums filling the vessel lumen, thin-walled cell lumen and even fibre cell lumen, reducing the space available for water invasion (Additional file). Furthermore, the BD of S1 and S2 was less than that of R1, with S2 exhibiting a notable decline, indicating a more pronounced degree of degradation. Similarly, in comparison to R2, the MWC of S3 had increased by 26.4%, while the BD had decreased by 17.3%. This suggested that S3 had undergone a significant degree of degradation.

Morphological analysis

The morphological structure is a key indicator that directly reflects the degree of degradation of waterlogged archaeological wood, as shown in Fig. 2. The waterlogged archaeological ebony samples exhibited minimal change in its micromorphological structure, with only minor cracks

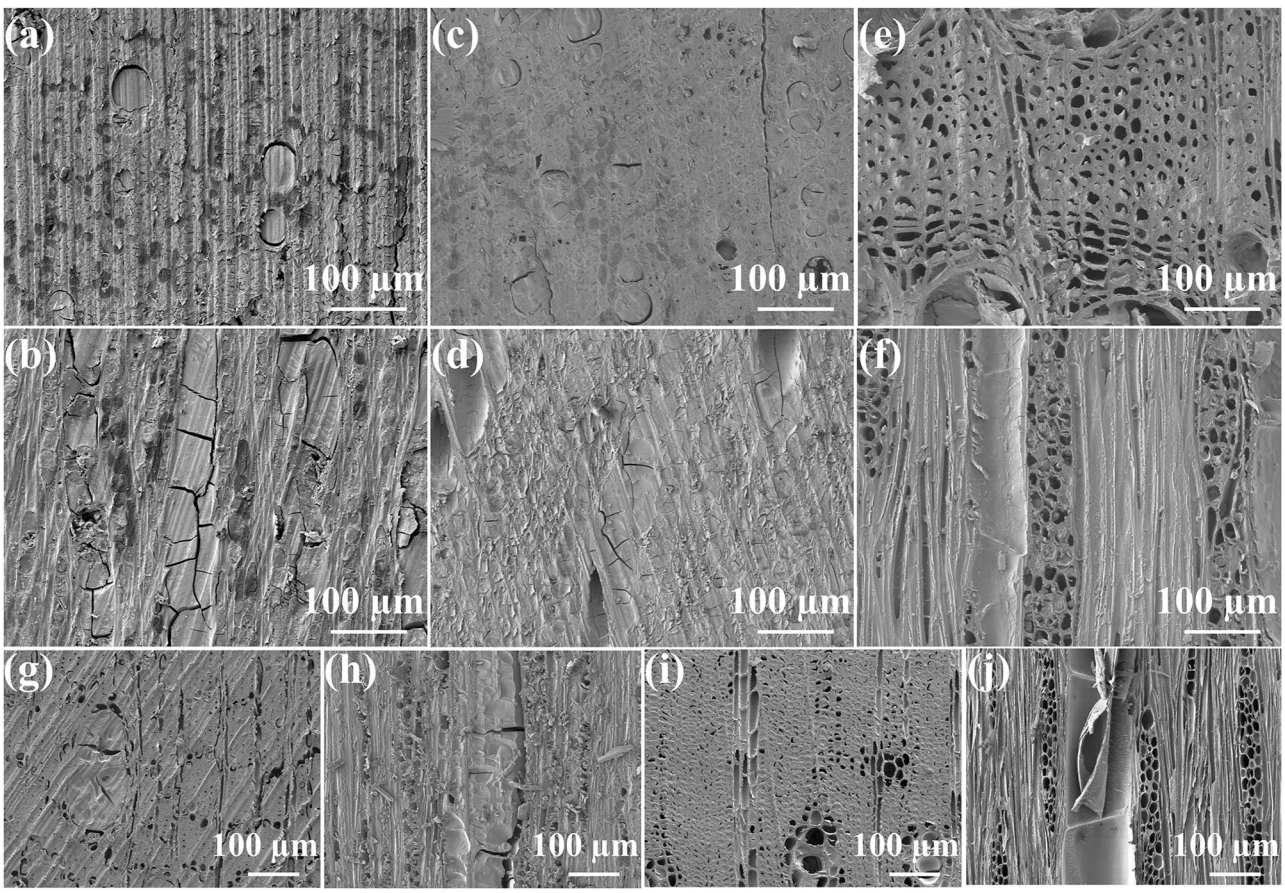

Fig. 2 | SEM images of transverse and longitudinal sections of waterlogged archaeological wood and reference wood. a, **b** S1, **c**, **d** S2, **e**, **f** S3, **g**, **h** R1, **i**, **j** R2.

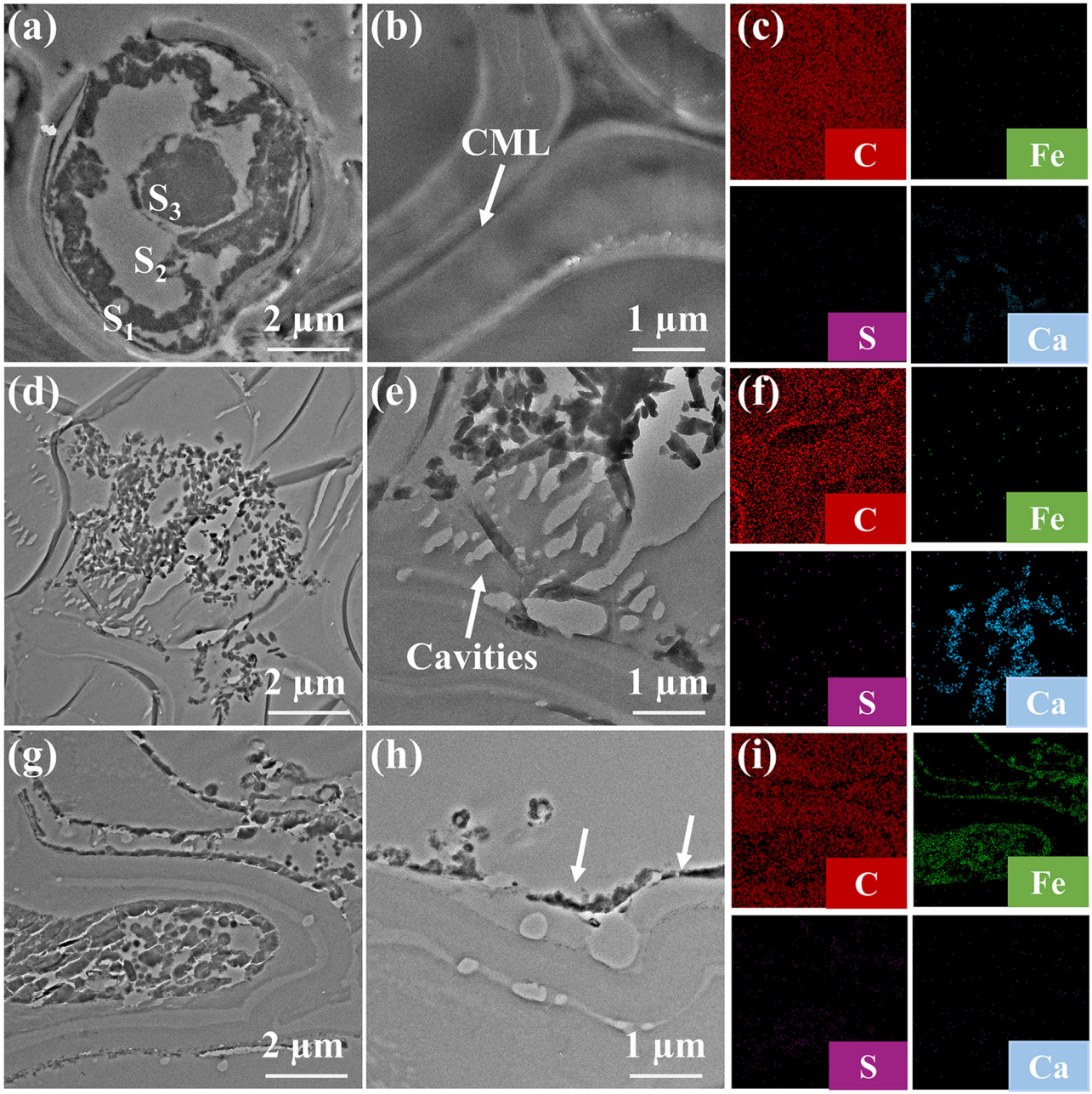

Fig. 3 | TEM images and energy dispersive spectrometer (EDS) images of waterlogged archaeological wood. a–c S1, **d–f** S2, **g–i** S3.

observed in some areas, which may have occurred during sample preparation (Fig. 2a–d). Moreover, the lumens of vessels and thin-walled cells, along with those of the fibre cells themselves, were replete with gums. This restricted potential routes for microbial penetration and also imparted intrinsic preservative properties to the ebony. This characteristic enabled the ebony to remain well-preserved even after being buried at sea for ~500 years. Furthermore, the morphological structure of sample S3 also demonstrated integrity (Fig. 2e, f). In comparison with sample R2, however, the cell walls appeared thinner, which could be attributed to microbial erosion. However, intraspecific differences might also contribute to this observation.

To minimize the damage incurred during the sample preparation process, we employed resin embedding and examined the degradation of waterlogged archaeological wood at the cellular level using a high-resolution TEM, as shown in Fig. 3. The secondary wall of the cell wall in sample S1 had experienced some degree of degradation, however, the CML and the cell wall corners remained relatively well preserved (Fig. 3a), primarily because of the higher lignin content in this area, which afforded greater resistance to microbial erosion[24]. Sample S2, located on the exterior of the log, was in poor condition, with its cell walls exhibiting a 'sieve-like' structure (Fig. 3d, e). This was likely due to the erosion of bacteria or soft rot fungi[12]. Furthermore, a considerable number of calcium salt particles were observed on the cell walls (Fig. 3d, f), which may be attributed to the penetration of calcium salts from seawater. In sample S3, which exhibited a higher degree of visible degradation, there were numerous small cavities on the cell walls, the cell walls were thin, and the damage was significant. Additionally, a significant amount of iron elements was found within the cell lumens and along the edges of the degraded cell walls (Fig. 3g, i). The presence of iron compounds was likely to accelerate the degradation process of wood[8]. Therefore, if the wreck is salvaged, the removal of iron salts must be considered.

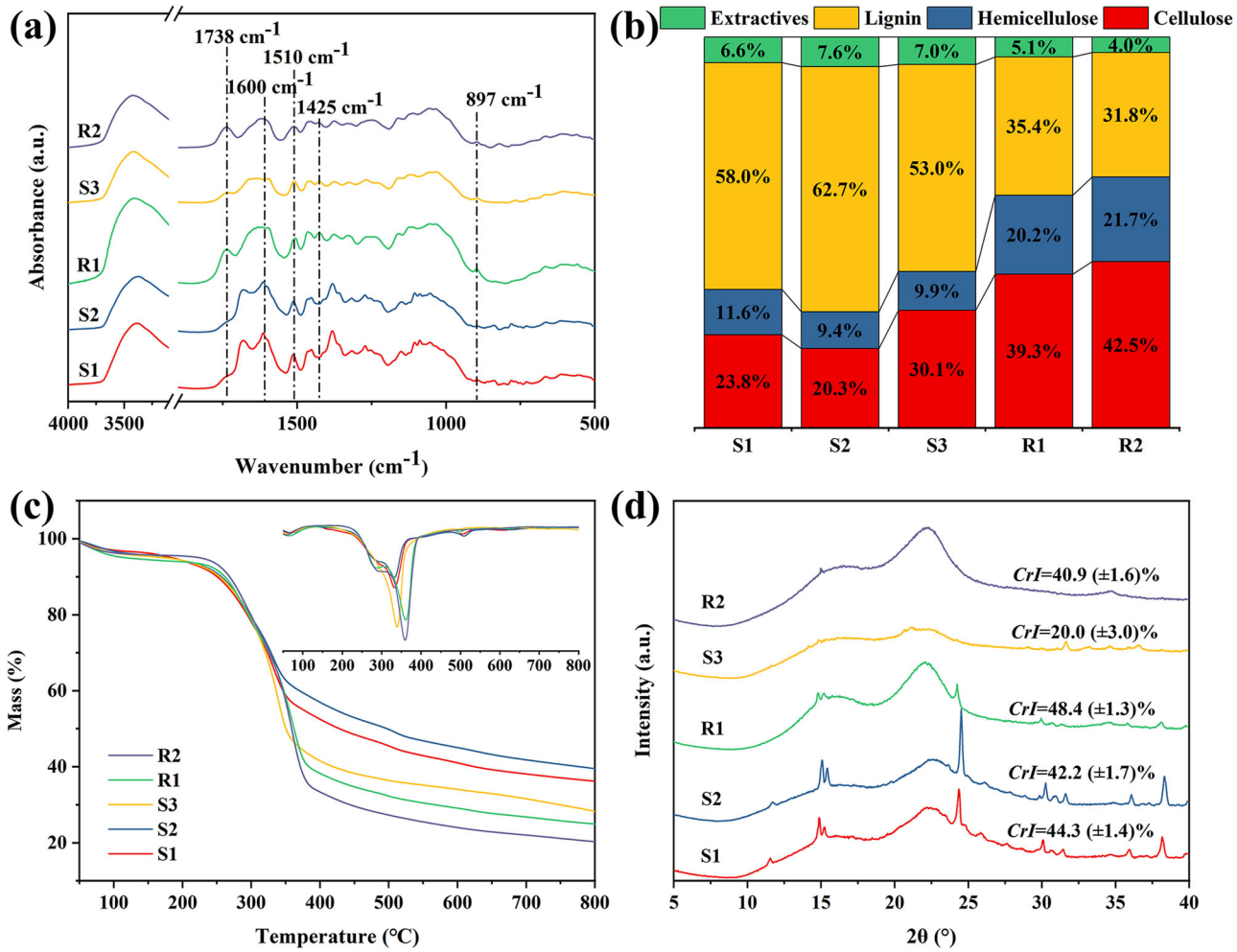

Fig. 4 | Analysis of chemical components of archaeological wood. a FTIR, **b** wet chemical analysis, **c** TG and DTG, **d** XRD.

Chemical analysis

Fourier transform infra-red spectroscopy (FTIR) was used to assess the degradation in waterlogged archaeological wood samples, as shown in Fig. 4a. The absorption peak at 1738 cm^{-1} is primarily attributed to the C=O stretching vibration of the acetyl group in hemicellulose[4]. In comparison to reference samples, the absorption peak's disappearance was evident in waterlogged archaeological wood samples, even in the seemingly well-preserved S1 sample. This indicated a significant degradation of the hemicellulose. The absorption peaks at 897 cm^{-1} and 1425 cm^{-1} are attributed to the anomeric carbon (C1) vibration of cellulose and the CH_2 scissoring vibration, respectively[4,25]. In comparison to reference wood samples, these peaks were diminished or absent in waterlogged archaeological wood, indicating cellulose degradation. The absorption peaks at 1510 cm^{-1} and 1600 cm^{-1} were attributed to the aromatic ring skeleton vibration of lignin[25]. Despite the degradation observed, the intensity of these peaks remained relatively constant compared to reference wood samples, suggesting the phenylpropane structure of lignin was stable and resistant to degradation or ring-opening reactions. This characteristic was the main reason the CML and cell wall corners in waterlogged archaeological wood cell walls remained intact.

Moreover, wet chemical analysis enables the quantitative evaluation of the primary chemical constituents in wood, facilitating the assessment of degradation in waterlogged archaeological wood[3]. As shown in Fig. 4b, the relative content of hemicellulose in the S1 and S2 samples was 11.6% and 9.4%, respectively, representing a decrease by 42.6% and 53.5% compared to the reference sample R1. The relative content of cellulose exhibited a decrease of 39.4% and 48.3%, respectively. In comparison to the reference sample R2, the relative content of hemicellulose and cellulose in the S3 sample exhibited a decrease of 54.4% and 29.2%, respectively. Due to the considerable reduction in the relative content of holocellulose, the relative content of lignin in the S1, S2 and S3 waterlogged archaeological wood samples had increased.

TG is a significant methodology for investigating alterations in wood composition. In contrast to wet chemical analysis, it requires a relatively small number of samples to reflect the three principal components of wood[26]. Figure 4c illustrates the TG and differential thermogravimetric (DTG) curves of the waterlogged and reference wood samples. Prior to 230 °C, the primary processes were volatilisation and decomposition of diverse forms of water, small molecular compounds and a small amount of hemicellulose. At temperatures between 230 °C and 300 °C, the primary process was the degradation of polymers, especially hemicellulose. In the temperature range of 300–390 °C, the degradation of cellulose and lignin was predominantly observed. At temperatures above 390 °C, the remaining lignin continued to degrade. At 390 °C, the mass loss of the S1 and S2 samples was 46.6% and 42.0%, respectively, while the mass loss of R1 was 60.8%. This suggested that both the S1 and S2 samples have undergone some degree of degradation, with the degree of degradation of the S2 sample being significantly greater than that of the S1 sample. From the DTG curve, it can be observed that in the temperature range of 230–300 °C, the S3 sample did not exhibit a peak, indicating that the degradation of hemicellulose in the S3 sample was significantly more severe than that observed in the R2 sample. At a temperature of 390 °C, the mass loss of the R2 sample was 65.7%, while

the mass loss of the S3 sample was 57.5%. The results showed that the cellulose and hemicellulose of waterlogged archaeological wood were subject to significant degradation. Furthermore, developing a model to assess the degradation status of archaeological wood using the TG technique is a promising area for future research.

The crystalline structure of cellulose can reflect its degradation state. Figure 4d illustrates the X-ray diffraction (XRD) patterns of the waterlogged archaeological and reference wood samples. Compared with R1 (CrI = 48.4%), the relative crystallinity of cellulose in the S1 and S2 samples exhibited a decline of 8.5% and 12.8%, respectively. This indicated the damage to both amorphous and crystalline regions of the cellulose in the archaeological ebony, with the S2 sample showing a significantly higher degree of degradation. Compared with R2 (CrI = 40.9%), the relative crystallinity of cellulose in the S3 sample decreased by 51.1%, which indicated that the cellulose has undergone severe damage. Furthermore, the absence of the (004) diffraction peak (2θ = 34.5) in S1, S2 and S3 in comparison to the reference wood samples suggested that the cellulose microfibrils in the archaeological wood have fragmented and become disoriented[8,9].

In conclusion, considering the intraspecific differences between the reference wood samples and the origin of the waterlogged archaeological wood, a series of chemical analyses of the components were conducted, including qualitative and quantitative experiments. The results consistently indicated that the hemicellulose and cellulose in the waterlogged archaeological wood have undergone some degree of degradation. Despite the apparent well-preserved condition of the S1 sample, its chemical components had undergone significant alterations. Consequently, it is clear that future preservation efforts must include physical or chemical protection measures.

Micromechanical properties

Wood is a natural polymer composite with multiple scales, with the cell wall serving as the solid material. The macroscopic mechanical properties of wood are largely determined by the mechanics of its cell walls[27]. Therefore, an in-situ nanoindentation system was employed to investigate the mechanical properties of the cell walls of waterlogged archaeological wood and reference samples, as illustrated in Fig. 5. In comparison to the control sample R1, the elastic modulus of the cell walls of S1 and S2 showed a decrease by 6.4% and 19.4%, respectively. The elastic modulus of the cell walls of S3 decreased by 15.6% compared to the reference sample R2. Consistently, the hardness of the cell walls of the waterlogged archaeological wood also showed a slight decrease compared to the reference samples. The high elastic modulus of cellulose, compared to other wood components, is the main factor affecting the longitudinal elastic modulus of the cell wall[10]. Thus, the reduction in elastic modulus was largely attributable to the degradation of cellulose. Furthermore, the degradation of hemicellulose and alterations in the lignin structure resulted in the rupture of intermolecular and intramolecular bonds, thereby weakening the interconnections between polymers within the wood cell wall[28]. Such changes ultimately led to a reduction in the load-bearing capacity of the cell walls of the waterlogged archaeological wood, as shown by a decline in both the elastic modulus and hardness. This method provides a new method for the mechanical evaluation of small volume wooden relics. In addition, strengthening the cell walls of salvaging wood before it is dehydrated is a crucial step. However, due to the unusually thick cell walls of the wood samples in the wreck, their permeability is extremely poor, which makes it difficult for traditional reinforcement methods to penetrate and work. Therefore, it is particularly urgent to develop a nano-scale reinforcement agent. This nano-type reinforcer is able to penetrate the wood cell wall more effectively, achieving deep reinforcement to protect the wood from further damage.

Microorganism identification

The deterioration of waterlogged archaeological wood is significantly influenced by the microorganisms in its surrounding environment. Accordingly, the microorganisms, including bacteria and fungi, present in the waterlogged archaeological ebony (S1 and S2), waterlogged archaeological Toona wood (S3) and the surrounding seabed sediment (E1) and bottom seawater (E2) were identified, as illustrated in Fig. 6. Figure 6a, b illustrate the bacterial species and relative abundance at the phylum and genus levels in the waterlogged archaeological wood and its surrounding environment. It was notable that there were differences in the dominant bacterial phyla among the various samples. Proteobacteria dominated with 94.53% in S1, 81.73% in S2, 80.61% in S3, 54.82% in E1 and 93.32% in E2. Many species within this phylum were capable of effectively degrading xylan[29]. Furthermore, Bacteroidetes also exhibited a relatively high abundance in the waterlogged archaeological wood and environmental samples. It was postulated that the bacteria in this phylum were capable of effectively degrading a variety of carbohydrate substances, including cellulose, pectin, mannan and xylan, among others[30]. It was worthy of particular note that the relative abundance of Desulfobacterota in the S3 sample was 6.87%. In the process of metabolising small organic molecules, some bacteria belonging to the Desulfobacterota were capable of utilising sulphate as an electron acceptor, reducing it to sulphide. Additionally, HS^- will undergo a reaction with iron, resulting in the production of iron sulphide. Iron sulphide was susceptible to oxidation in the presence of water, resulting in the production of sulphuric acid. The

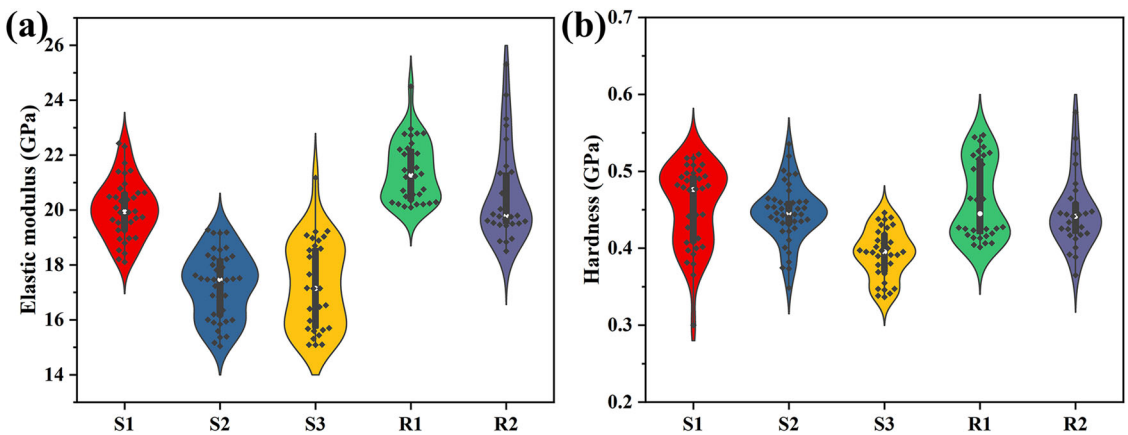

Fig. 5 | Cell wall mechanical properties of archaeological wood and reference samples. a Elastic modulus, **b** Hardness.

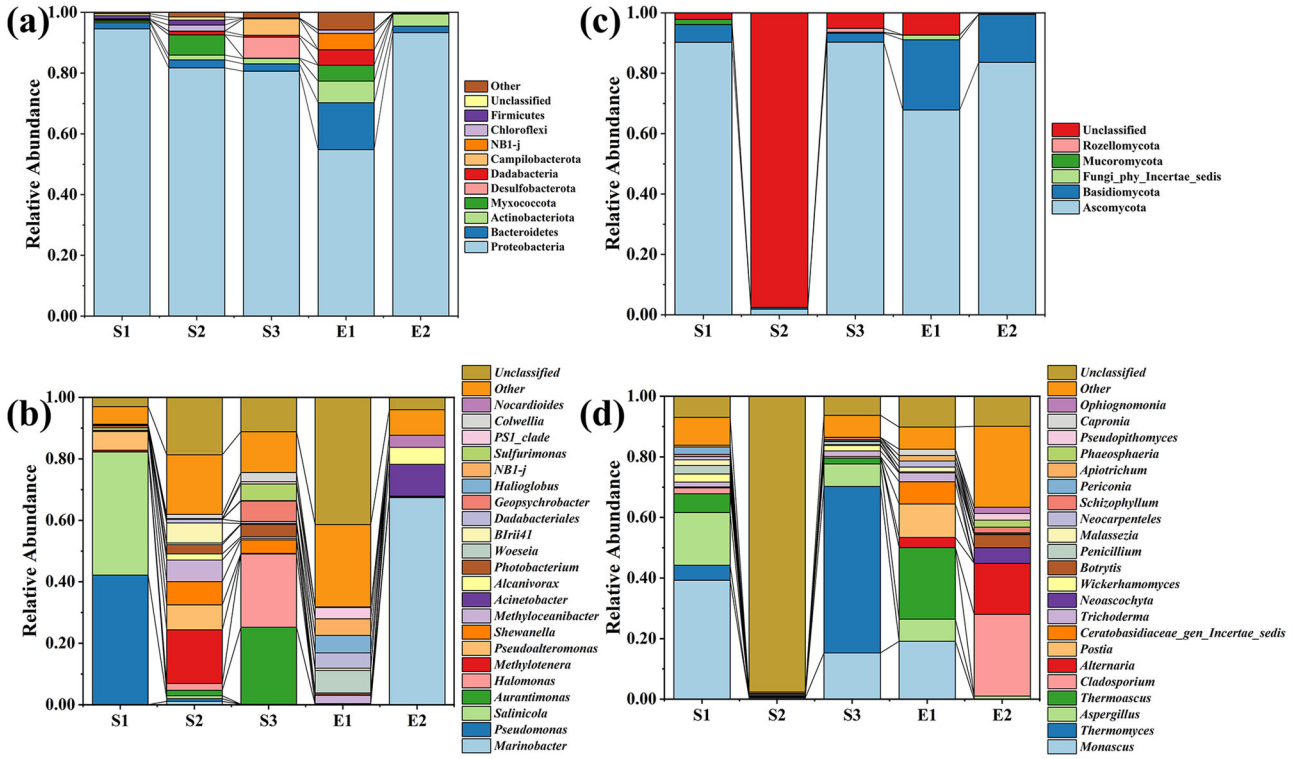

Fig. 6 | Bacteria and fungi in waterlogged archaeological wood and its surrounding environment. a, **b** Bacterial species and relative abundance at the phylum and genus levels, **c**, **d** Fungal species and relative abundance at the phylum and genus levels.

objective was to facilitate the further degradation of the already hemicellulose and cellulose in wood[8,31]. Previous studies had identified a high concentration of Fe elements in S3 samples. Therefore, strategies for the removal of iron sulphide should be explored in future research to mitigate its impact on wood degradation.

Figure 6c shows the fungal species at the phylum level, while Fig. 6d illustrates their relative abundance at the genus level in the waterlogged archaeological wood and its surrounding environment. Unlike bacteria, fungi exhibited a relatively lower biodiversity in the waterlogged archaeological wood and its surrounding environment, likely due to the anoxic conditions. The main fungal phyla present were Ascomycota and Basidiomycota. Most of the soft rot fungi in waterlogged archaeological wood belonged to Ascomycetes. At the genus level, *Monascus*, *Thermomyces* and *Aspergillus* were identified as the main dominant fungal genera. They could secrete enzymes that cause wood degradation and discoloration[17].

Figure 7 illustrates the diversity of microbial communities in waterlogged archaeological wood and its surrounding environment to explore the correlation between the environment and the microorganisms of the waterlogged archaeological wood samples. Among bacteria, there were 21 distinct OTUs shared across different samples (Fig.7a). Among fungi, only 2 shared OTUs were observed. (Fig.7b). The unweighted UniFrac, which considers only the presence or absence of species in the samples, and the weighted UniFrac, which takes into account both the presence of species and their abundance, have distance values ranging from 0 to 1. A value of 0 indicates that there is no difference in the microbial communities between two samples, and the closer the value is to 1, the greater the difference between the microbial communities of the two samples. Figure 7c–f demonstrate that, despite sample differences, the microbial communities appeared to occupy similar ecological niches. Therefore, the microbial community on waterlogged archaeological wood was closely related to the environment in which it is located.

Conclusion

This study employed an interdisciplinary approach to examine the degradation of waterlogged archaeological wood from the Second Shipwreck Site on the northwestern continental slope of the South China Sea, focusing on the multi-scale structure of wood. Utilised molecular biological methods further explored the microbial community characteristics of the wood and its surrounding environment. The study revealed that the wood had undergone varying degrees of degradation, with signs including damage to the secondary wall, degradation of hemicellulose and cellulose and disordered arrangement of cellulose microfibrils. Applying in-situ nanoindentation technology, this research assessed the micro-mechanical properties of the wood, finding that the elastic modulus and hardness of the cell walls had significantly degraded compared to undeteriorated wood. The microbial community was dominated by bacteria, which is closely related to the anaerobic environment. A significant correlation existed between the microbes in the wood and those in the surrounding environment. The well preservation of logs in shipwrecks can be attributed to their inherent structural properties, including a large amount of gum filling and their extremely thick cell wall structure. However, with the passage of time, deterioration is inevitable, so it is necessary to salvage and protect the wood in the wreck. Notably, a large amount of iron salts detected in some wood may accelerate degradation, suggesting that their removal was critical for conservation. Furthermore, it has been observed that the outermost layer cell walls of the pile have undergone a degree of degradation, necessitating reinforcement prior to the dehydration process to prevent the collapse of the cell walls due to water loss. Effective preservatives are essential for not only eliminating and preventing anaerobic bacteria but also for protecting against the decay caused by fungi after the wreck has been salvaged. This study provided a scientific basis for understanding the deterioration mechanisms of waterlogged archaeological wood and laid the foundation for its conservation and restoration, contributing new technical methods and theoretical insights like micromechanical testing and TG analysis for the field of archaeological wood deterioration research.

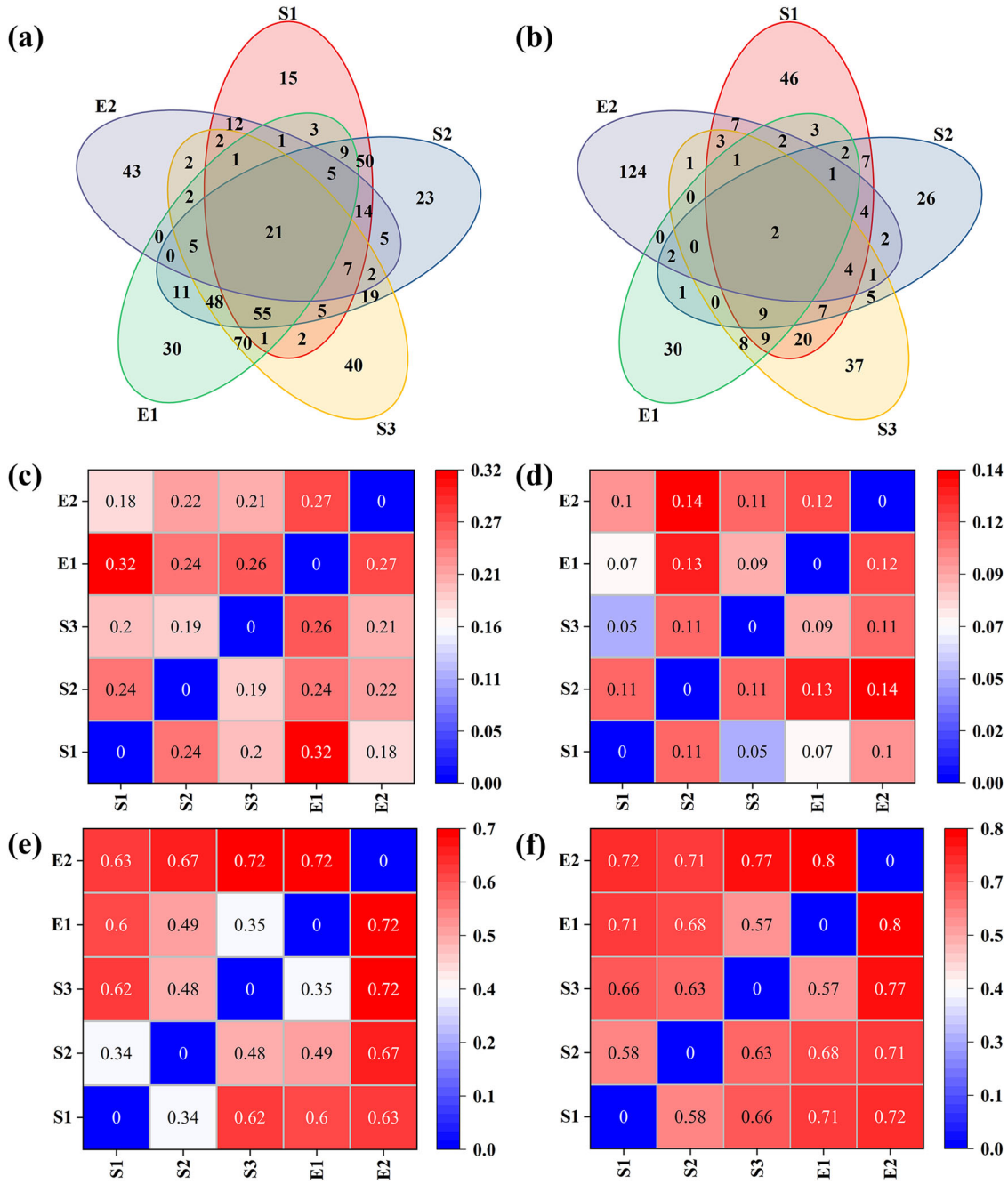

Fig. 7 | The microbial community correlation of waterlogged archaeological wood and its surrounding environment. a, b Veen diagrams of bacterial and fungal OTUs, **c, d** Heat maps of weighted UniFrac bacterial and fungal beta diversity, **e, f** Heat maps of unweighted UniFrac bacterial and fungal beta diversity.

Data availability

No datasets were generated or analysed during the current study.

Abbreviations

MWC	Maximum water content
BD	Basic density
SEM	Scanning electron microscope
TEM	Transmission electron microscopy
PCR	Polymerase chain reaction
DNA	Deoxyribonucleic acid
SPSS	Statistical package for the social sciences
CML	Compound middle lamella
EDS	Energy dispersive spectrometer
FTIR	Fourier transform infra-red spectroscopy
TG	Thermogravimetric
DTG	Differential thermogravimetric
XRD	X-ray diffraction

Received: 24 September 2024; Accepted: 24 November 2024;
Published online: 11 February 2025

References

1. Björdal, C. G., Nilsson, T. & Daniel, G. Microbial decay of waterlogged archaeological wood found in Sweden. *Int. Biodeterior. Biodegrad.* **43**, 63–73 (1999).

2. Singh, A. P., Kim, Y. S. & Chavan, R. R. Advances in understanding microbial deterioration of buried and waterlogged archaeological woods: a review. *Forests* **13**, 394 (2022).
3. Chu, S., Lin, L., & Wang, D. Multi-scale structural deterioration analysis of archaeological wood from the Shahe Ancient Bridge site in Xi'an, Shaanxi, China. *Wood Mater Sci. Eng*. https://doi.org/10.1080/17480272.2024.2380875 (2024).
4. High, K. E. & Penkman, K. E. H. A review of analytical methods for assessing preservation in waterlogged archaeological wood and their application in practice. *Herit. Sci.* **8**, 83 (2020).
5. Kim, J. S. et al. Characterization of microbial decay and microbial communities in waterlogged archaeological rosewood (Dalbergia species). *Forests* **14**, 1992 (2023).
6. Chen, C. et al. Structure-property-function relationships of natural and engineered wood. *Nat. Rev. Mater.* **5**, 642–666 (2020).
7. Tamburini, D. et al. A critical evaluation of the degradation state of dry archaeological wood from Egypt by SEM, ATR-FTIR, wet chemical analysis and Py(HMDS)-GC-MS. *Polym. Degrad. Stab.* **146**, 140–154 (2017).
8. Wang, D., Dong, W., Cao, L., Zhu, C. & Yan, J. Deterioration mechanisms of archaeological wood inside the bronze parts of excavated chariots from the Western Han dynasty. *J. Cult. Herit.* **62**, 90–98 (2023).
9. Guo, J. et al. Molecular and crystal structures of cellulose in severely deteriorated archaeological wood. *Cellulose* **29**, 9549–9568 (2022).
10. Chu, S., Lin, L., Zhang, Y. & Wang, D. Physicochemical structure and micromechanical properties of archaeological wood under alternating dry and wet conditions. *Wood Mater. Sci. Eng.* **19**, 691–701 (2023).
11. Wang, B., Qi, M., Ma, Y., Zhang, B. & Hu, Y. Microbiome diversity and cellulose decomposition processes by microorganisms on the ancient wooden seawall of Qiantang River of Hangzhou, China. *Micro. Ecol.* **86**, 2109–2119 (2023).
12. Lu, Y. et al. Preservation status and microbial community of waterlogged archaeological woods over 7800 years old at the Jingtoushan Site, China. *Wood Sci. Technol.* **57**, 537–556 (2023).
13. Björdal, C. G. & Elam, J. Bacterial degradation of nine wooden foundation piles from Gothenburg historic city center and correlation to wood quality, environment, and time in service. *Int. Biodeterior. Biodegrad.* **164**, 105288 (2021).
14. Cha, M. Y., Lee, K. H., Kim, J. S. & Kim, Y. S. Variations in bacterial decay between cell types and between cell wall regions in waterlogged archaeological wood excavated in the intertidal zone. *IAWA J.* **42**, 457–474 (2021).
15. Pedersen, N. B., Łucejko, J. J., Modugno, F. & Björdal, C. Correlation between bacterial decay and chemical changes in waterlogged archaeological wood analysed by light microscopy and Py-GC/MS. *Holzforschung* **75**, 635–645 (2021).
16. Gjelstrup Björdal, C. Microbial degradation of waterlogged archaeological wood. *J. Cult. Herit.* **13**, S118–S122 (2012).
17. Walsh-Korb, Z. & Avérous, L. Recent developments in the conservation of materials properties of historical wood. *Prog. Mater. Sci.* **102**, 167–221 (2019).
18. Singh, A. P. et al. Relationship of wood cell wall ultrastructure to bacterial degradation of wood. *IAWA J.* **40**, 845–870 (2019).
19. Liu, S., Ran, Y. & Cao, J. Comparison on thermally modified beech wood in different mediums: Morphology, chemical change and water-related properties. *Ind. Crop Prod.* **209**, 117935 (2024).
20. Segal, L., Creely, J. J., Martin, Jr. A. E. & Conrad, C. M. An empirical method for estimating the degree of crystallinity of native cellulose using the X-ray diffractomete. *Text. Res J.* **29**, 786–794 (1959).
21. Pizzo, B., Pecoraro, E. & Lazzeri, S. Dynamic mechanical analysis (DMA) of waterlogged archaeological wood at room temperature. *Holzforschung* **72**, 421–431 (2018).
22. Dong, G. et al. The deterioration state and degradation mechanism of historical timber structures from the Yunnan Military Academy. *Wood Mater. Sci. Eng.* **18**, 1878–1887 (2023).
23. Babiński, L., Izdebska-Mucha, D. & Waliszewska, B. Evaluation of the state of preservation of waterlogged archaeological wood based on its physical properties: basic density vs. wood substance density. *J. Archaeol. Sci.* **46**, 372–383 (2014).
24. Traoré, M., Kaal, J. & Martínez Cortizas, A. Application of FTIR spectroscopy to the characterization of archeological wood. *Spectrochim. Acta Part A* **153**, 63–70 (2016).
25. Pandey, K. K. & Pitman, A. J. FTIR studies of the changes in wood chemistry following decay by brown-rot and white-rot fungi. *Int. Biodeterior. Biodegrad.* **52**, 151–160 (2003).
26. Chen, M., Ma, Y., Zhang, B. & Hu, Y. Feasibility study on conservation of water-saturated archaeological wood in earthen sites by hot air with different humidity. *Eur. Phys. J.* **139**, 55 (2024).
27. Qin, L., Lin, L., Fu, F. & Fan, M. Micromechanical properties of wood cell wall and interface compound middle lamella using quasi-static nanoindentation and dynamic modulus mapping. *J. Mater. Sci.* **53**, 549–558 (2017).
28. Eder, M., Arnould, O., Dunlop, J. W. C., Hornatowska, J. & Salmén, L. Experimental micromechanical characterisation of wood cell walls. *Wood Sci. Technol.* **47**, 163–182 (2012).
29. Parab, P. D., Khandeparker, R. D., Shenoy, B. D. & Sharma, J. Phylogenetic diversity of culturable marine bacteria from mangrove sediments of goa, india: a potential source of xylanases belonging to glycosyl hydrolase family 10. *Appl. Biochem. Microbiol.* **56**, 718–728 (2020).
30. Zheng, R., Cai, R., Liu, R., Liu, G. & Sun, C. Maribellus comscasis sp. nov., a novel deep-sea Bacteroidetes bacterium, possessing a prominent capability of degrading cellulose. *Environ. Microbiol.* **23**, 4561–4575 (2021).
31. Fors, Y. et al. Sulfur and iron analyses of marine archaeological wood in shipwrecks from the Baltic Sea and Scandinavian waters. *J. Archaeol. Sci.* **39**, 2521–2532 (2012).

Acknowledgements

The authors express their gratitude to Bei Luo from Southwest Forestry University for their assistance with this study. This work was supported by the National Social Science Fund of China for Post-funding and Excellent Doctoral Dissertation Publishing Project (23FKGA002).

Author contributions

The manuscript was prepared through contributions of all authors. S.C. carried out the experiments, conducted all data analysis and wrote most of the manuscript. Y.L. carried out the experiments. N.L., X.W. and J.S. provided experimental samples, defined the research project. L.L. designed the experiments. All authors have given approval to the final version of the manuscript.

Competing interests

The authors declare no competing interests.

Additional information

Supplementary information The online version contains supplementary material available at https://doi.org/10.1038/s40494-025-01628-8.

Correspondence and requests for materials should be addressed to Xueyu Wang or Naisheng Li.